Microstructure and Its Relationship to Deformation Processes in Amorphous Polymer Glasses

STEPHEN T. WELLINGHOFF and ERIC BAER, *Department of Macromolecular Science, Case Western Reserve University, Cleveland, Ohio 44106*

Synopsis

The microdeformation morphology of a number of vinyl polymers with bulky side chains (type I) and arylene polymers with flexible oxygen linkages (type II) was studied by electron microscopy. The polyarylenes crazed only near the glass transition while the polyvinyls exhibited a crazing regime that extended to liquid nitrogen temperatures. In addition significantly less plastic strain was localized in type II glass crazes relative to those in type I glasses. In compatible blends of polystyrene (PS) and 2,6-dimethyl poly(phenylene oxide) (2MPPO), ca. 30% 2MPPO was sufficient to induce a transition from type I to type II crazing behavior. Small amounts of PS suppressed the low-temperature 2MPPO β relaxation but enhanced the intermediate transition of 2MPPO at higher temperatures. Blending increased the conformational energy of the 2MPPO chain and improved interchain packing. The propensity for the polymer glass to form sharp shear bands at the expense of diffuse bands was increased by a decrease in the conformation energy of the polymer chain and an improvement in the glassy state packing.

INTRODUCTION

In recent years it has been found that polymers containing main chain aryl units connected by flexible heteroatom linkages (type II) are quite ductile in their amorphous glassy state. Polycarbonate of bisphenol A (PC), poly(ethylene terephthalate) (PET), and 2,6-dimethyl polyphenylene oxide (2MPPO) all exhibit considerable ductility.[1,2] The special features of the glassy microstructure responsible for the increased fracture resistance of these materials relative to vinyl polymers (type I) such as polystyrene (PS)[3] and poly(methyl methacrylate) (PMMA)[4] are still to be elucidated.

The presence of a main-chain sub-T_g β relaxation that is uncoupled from side chain motions is a common feature found in the tough amorphous thermoplastics. Brittle vinyl polymers apparently do not have such a relaxation process.[5] However, it is interesting to note that poly(vinylchloride) (PVC), which is quite ductile over a large temperature range, does exhibit a significant main-chain β relaxation.[6,7] Kastelic and Baer[1] have determined that the presence of this relaxation in PC and PET is responsible for the low-temperature shear ductility in these glasses. However, studies by Wysgoski and Yeh[8] have shown that ductility in PC at 25°C is increased when the β relaxation is suppressed and the higher temperature "intermediate" relaxation is enhanced by the addition of low molecular weight diluents. The β relaxation is only marginally affected by the glass enthalpy which can be decreased by sub-T_g annealing. But the intermediate transition decreases in intensity and increases in temperature upon annealing. In both type I and type II glasses annealing increases the propensity of the glass to develop plastic instability in the form of crazes or microshear

bands.[9,10] Obviously there is no simple correlation between relaxation processes and ductility.

The shear activation volume appears to have a more direct relationship to ductility. The shear activation volumes of type II glasses such as PC,[11] PET,[12] and 2MPPO[2] are from two to three times larger than the activation volumes of type I PS and PMMA glasses.[13,14] Argon and Bessanov[15] have also found that a number of aromatic polyimides with activation volumes three to eight times larger than that of PS behaved as type II glasses. Application of Argon's yield theory[16] to those results enabled these authors to conclude that the stress activation event in type II glasses was delocalized over a bundle of five to ten chains that move cooperatively. Only one chain contributed to the activation volume in type I glasses.

Electron microscopy of the surfaces of a number of type II glasses has revealed the presence of bundle-like structures (nodules) that move as units when the material is strained.[17-20] There is even some evidence that this structure is present in PS thin films[21] although the evidence must be considered less convincing in this case. The nodules are thought to be areas of higher packing density and are found to increase in size when the glass enthalpy is decreased.[19] Recently there has been attempt to correlate the nodular structure with the mechanical properties of PC.[19]

Neutron and x-ray diffraction experiments have tended to discount the presence of distinct nodular regions in the interior of thick films.[22,23] However, direct structural measurements have yet to reveal whether or not the interior of type II glasses deforms inhomogeneously by a slip mechanism involving bundle-like units. In any case surface nodules could have a profound influence upon the craze nucleation which involves a highly localized surface plastic deformation process.[24]

PS and PC possess significant differences in their craze morphology. Solvent crazes induced in PC at room temperature resemble micronecks with an internal lamellar structure oriented perpendicular to the craze growth direction.[8,25] Voiding occurred only at very high strain levels.[25] Although nascent PS crazes resemble micronecks they soon cavitate to form a highly fibrillated structure. Crazes nucleated in a PC sample whose β relaxation and intermediate transition had been suppressed by the addition of antiplasticizer were morphologically very similar to PS crazes.[8]

The preceding discussion suggests that amorphous glassy polymers can be classified into two groups (type I, type II) according to their general mechanical behavior. The craze initiation and growth process in a brittle vinyl polymer with a bulky side groups (type I), for example, PS, has been characterized in a previous article.[24] In this work the effect of glass enthalpy, molecular weight, and deformation temperature upon the shear band and craze morphology of PC glasses (type II) is explored in detail.

In addition, compatible blends[44] of a type II polymer, 2MPPO, and a type I polymer, PS, are studied. This system presents a unique opportunity to study the changes in glassy state microstructure that are responsible for the change between type I and type II mechanical properties. The effect of chemical composition, tacticity, and molecular weight upon the microdeformation morphology and the dynamic mechanical properties of the blend are considered. A preliminary account of this work has already been published.[26] The hope is that

a more detailed understanding of the molecular processes responsible for plastic deformation in amorphous polymer glasses will arise from a comparison of the microdeformation morphology found in the two types of polymer.

EXPERIMENTAL

Additive free, narrow-fraction PC samples (M_v = 11,000 and 30,000; General Electric Co.) or Lexan PC (M_v = 40,000; General Electric Co.) were dissolved in a mixture of dichloroethane and trichloroethylene. PS (M_n = 37,000; M_w/M_n ≅ 1.05; Pressure Chemical Co.) and atactic poly(p-tert-butylstyrene) (t-BPS) (M_v = 325,000; Dow Chemical Co.) were dissolved in xylene. The t-BPS used was purified by precipitation into methanol. Narrow molecular weight fraction APS (M_n = 37,000; 97,500; M_w/M_n ≅ 1.05; Pressure Chemical Co.) and a very high molecular weight APS (M_n ≅ 2,000,000, all molecular weights ≥670,00; Dow Chemical Co.) were mixed with an additive-free 2MPPO (M_v ≅ 25,000; General Electric Co.) in the desired portions in xylene to form a blend solution. IPS (M_w ≅ 2,000,000) blend solutions were also prepared. The IPS used was purified by precipitation into methanol and subsequently shown by IR to be ~100% isotactic.

These solutions were solvent cast upon an FEP (du Pont Co.) copolymer substrate after the substrate surface had been activated by Tesla coil discharge. A 3 × 3 mm 3000-Å-thick section of polymer film was isolated on the substrate by dissolving away the surrounding polymer film. A 2.5-cm-wide section of the substrate film was placed in the grips of a manual uniaxial tensile stretcher so as to center the thin square of polymer film between the grips and the substrate-free edges. The initial separation between the grips was set at 2.0 cm.

The PC, t-BPS, and blend films were then heated to 250°C under vacuum for 45 min to 1 hr to remove the traces of solvent and destroy any crystallinity. The PS could not be heated to such a high temperature since it would form droplets on the substrate surface. After air quenching to room temperature the films were annealed at T_g + 5°C for 4 hr under vacuum and slowly cooled to room temperature to remove interfacial stresses between the polymer thin film and the substrate. Literature values for the compositional dependence of the blend T_g were used.[27] The tacticity of the PS component was assumed not to affect the T_g.[28] The T_g values of the PS, t-BPS, and PC films were taken as 100°C,[5] 145°C,[5] and 145°C,[20] respectively. PC films were annealed at 130°C for either ½ hr, 30 hr, or 60 hr in order to prepare glasses with different enthalpies.

The FEP substrate deformed in a uniform fashion at all temperatures between −195° and 250°C. As a consequence it was possible to study the microdeformation morphology over a wide temperature range. A strain of 4% at −195°C and 10% at all higher temperatures was applied at a strain rate of 10^{-2}/sec.

Either gold decoration preceded or Pt–C shadowing followed deformation in a helium atmosphere. Subsequently, the films were carbon coated and stripped from the substrate with poly(acrylic acid) (PAA). The 3000-Å-thick films were observed directly in the transmission electron microscope after dissolution of the PAA. However, the ca. 10,000-Å-thick films were opaque to the electron beam. Therefore, the polymer layer was dissolved away from the replica by chloroform so that the replicated surface features could be observed. The surface nodular structure in the PC thin films was revealed by etching the polymer surface with 0.5% NaOH solution prior to Pt–C shadowing.[18]

Films of 2,6-diphenyl (2PPPO) and 2,6-methylphenyl poly(phenylene oxide) (2MPPPO) were prepared for electron microscopy in virtually the same way as the blend thin films. However, a few changes in casting and thermal treatment should be noted. Because of the rapid crystallization from xylene solution, 2PPPO was cast from sym-tetrachloroethane. The film was then heated to 200°C for 1 hr and slow cooled to room temperature. No further thermal treatment was employed. MPPPO films were prepared in exactly the same fashion as the blends. The annealing treatment for this polymer was 165°C for 4 hr.

Torsion pendulum measurements were performed at 1 Hz on 10-mil-thick specimens of APS–2MPPO and IPS–2MPPO blends. The blends were prepared by precipitating a xylene solution of the two polymers into methanol and compression molding the resulting powders into clear amorphous films under helium gas. All IPS blends were quenched from 260°C into water to prevent crystallization. APS blends were slow cooled to room temperature.

RESULTS AND DISCUSSION

Shear-to-Craze Transition—Effect of Chemical Structure and Glass Enthalpy

Figures 1 and 2 show thin films of PS and tBPS (type I) that have been deformed in an inert He atmosphere at a variety of temperatures. tBPS crazes over the entire temperature regime between T_g and $-195°C$. PS behaves in a similar way. The crazes are quite thin (ca. 600 Å wide) and have undergone significant voiding and fibrillation.

The high-temperature shear to craze transition temperature that occurs in
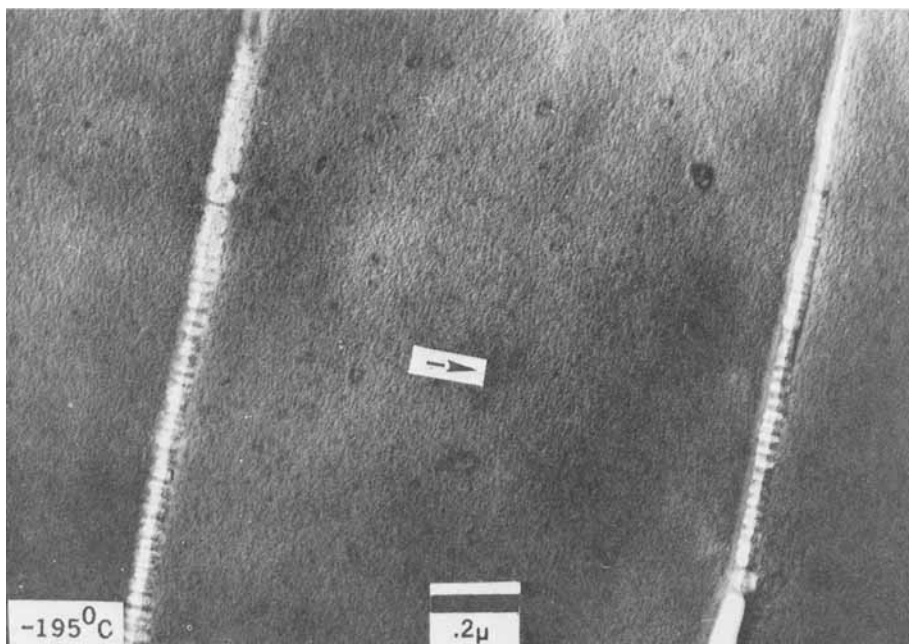

Fig. 1. Craze morphology in PS deformed 4% under He at the temperature indicated in the insert (Pt–C shadowed at 45° angle, C coated).
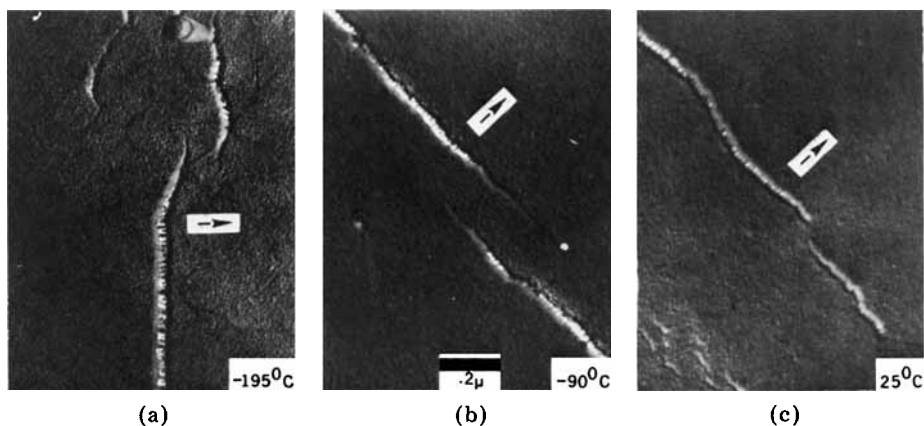
Fig. 2. Craze morphology in tBPS deformed 4% under He (Pt–C shadowed at 45° angle, C coated).

PC (type II) is shown in Figures 3 and 4. There is a strong effect of glass enthalpy upon both the temperature of the shear to craze transition and the amount of strain localized within shear bands. PC samples of molecular weights 30,000 and 11,000 behaved in a similar way. Sharp shear bands develop profusely in the 30 hr-annealed glass at both 100° and 125°C, Figures 3(b) and 3(c), arrows S.

The ca. 5000-Å-wide crazes that develop in the 30 hr-annealed glass consist of a collection of small nuclei 200–300 Å in width and 1000 Å in length. Isolated craze nuclei can be found at the intersection of the shear bands in Figure 4(b), arrow C; because of the stress relaxation in the elastically deformed matrix adjacent to and behind the shear band growth tip, the nucleus does not develop into a mature craze. In general, shear bands stop craze growth.[45] These structures are undoubtedly similar to the craze nuclei found in PS.[24] However, when compared to PS, the formation of a craze in PC appears to involve the coalescence of many more of these nuclei perpendicular to the craze growth direction.
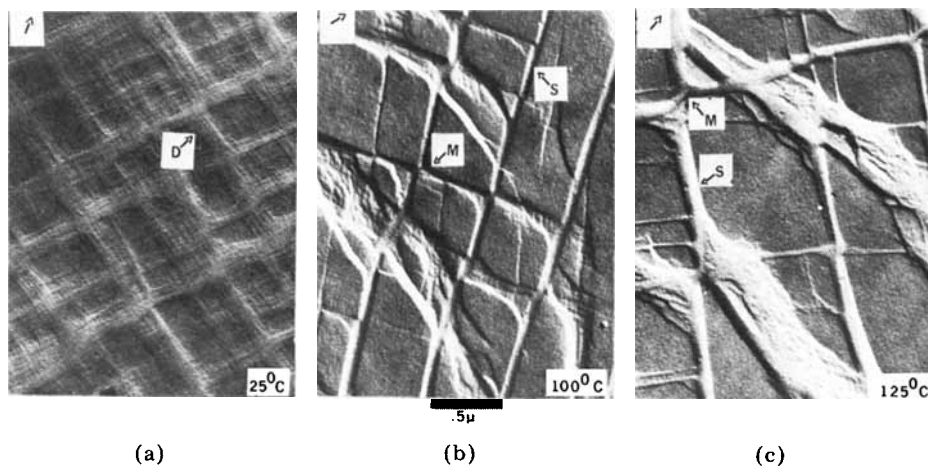

Fig. 3. Shear-to-craze transition and extensive shear strain localization in PC (MW 40,000), annealed for 30 hr at 130°C and deformed 10% (Pt–C shadowed at 30° angle, C coated).
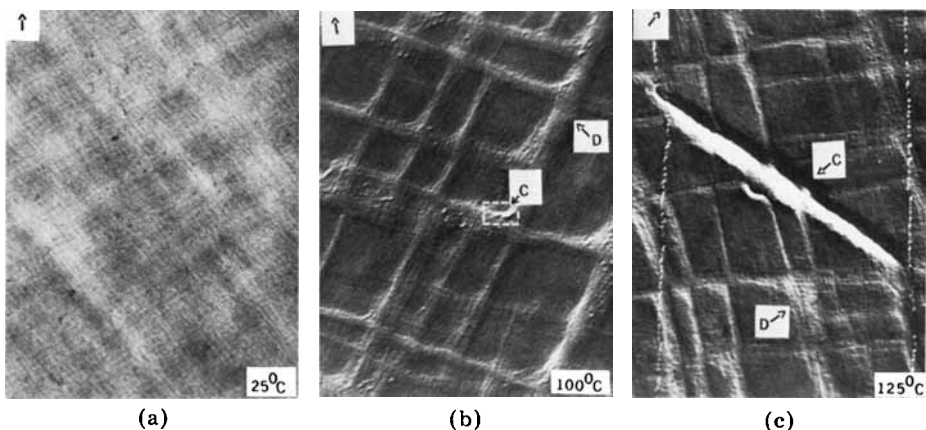
Fig. 4. Same as Figure 3, except annealed for ½ hr at 130°C. Shows a more diffuse shear deformation.

At 25°C no crazes can be found and a finer more diffuse shear morphology appears, Figure 3(a). Fine bands (ca. 100 Å thick) that grow in both the maximum shear directions have a tendency to collect and localize the shear deformation into ca. 3000 Å-wide diffuse shear bands, Figure 3(a), arrow D.

The fine bands are less distinct and more delocalized in the high-enthalpy glass deformed at 25°C. As the temperature of deformation is increased to 100–125°C the fine bands collect into diffuse shear bands, Figures 4(b) and 4(c), arrows D; a number of sharp bands can also be observed at these temperatures, Figure 4(c), arrows S. Isolated craze nuclei form at 100°C, Figure 4(b), arrow C; but the coalescence of the nuclei into mature crazes can be seen at 125°C, Figure 4(c), arrow C.

Figure 5 shows the shear-to-craze transition that takes place in 2MPPO at ca. 140°C. At room temperature diffuse shear bands nucleate throughout the entire solid, Figure 5(b), D. These fine shear bands are less distinct at −90°C, and a block-like shear structure is more apparent, Figure 5(a). Sharp shear bands and
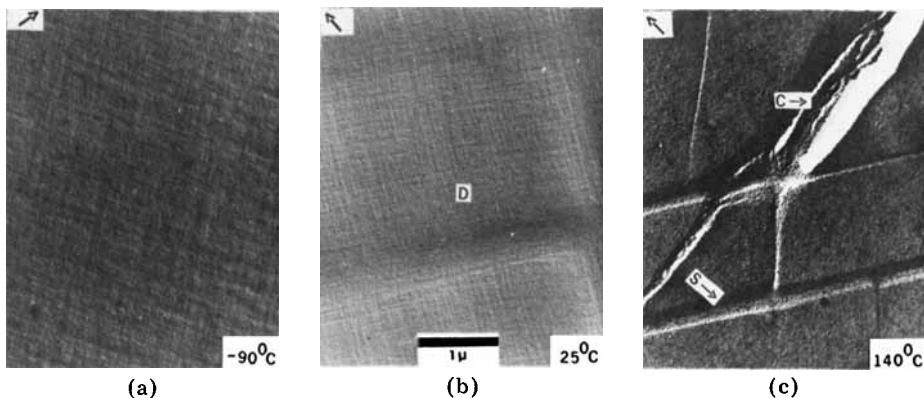

Fig. 5. Pt–C replica of the shear band and craze morphology in ca. 10,000-Å-thick films of 2MPPO—the effect of deformation temperature. Films deformed 10% (Pt–C shadowed at 30° angle, C coated).

crazes are observed at 140°C, Figure 5(c), arrows S and C.   In both PC and 2MPPO an increase in the temperature of deformation increases the propensity to shear in a localized fashion.   The effect of temperature on the shear defor-mattion morphology is quite different from polymers with high PS contents.

Symmetrically 2,6-disubstituted PPOs such as the dimethyl and diphenyl polymers have low-temperature β relaxations that involve backbone reorienta-tion.[30]   However, this relaxation process does not appear in asymmetrically substituted PPOs (e.g. 2-methyl 6-phenyl PPO).[30]

The microdeformation morphologies of the diphenyl and dimethyl PPOs are typical of type II polymers (Figs. 5 and 6).   Both deform by diffuse shear banding at low temperatures and undergo shear-to-craze transitions at high temperature. On the other hand, 2-methyl 6-phenyl PPO forms sharp shear bands at all temperatures (Fig. 7).   Diffuse shear bands are nonexistent.   No distinct shear-to-craze transition is observed above −90°C.   Thus, even though this polymer's backbone is similar to the other PPOs, its mechanical properties are quite different.   The thermal expansion coefficient of the asymmetric PPO is
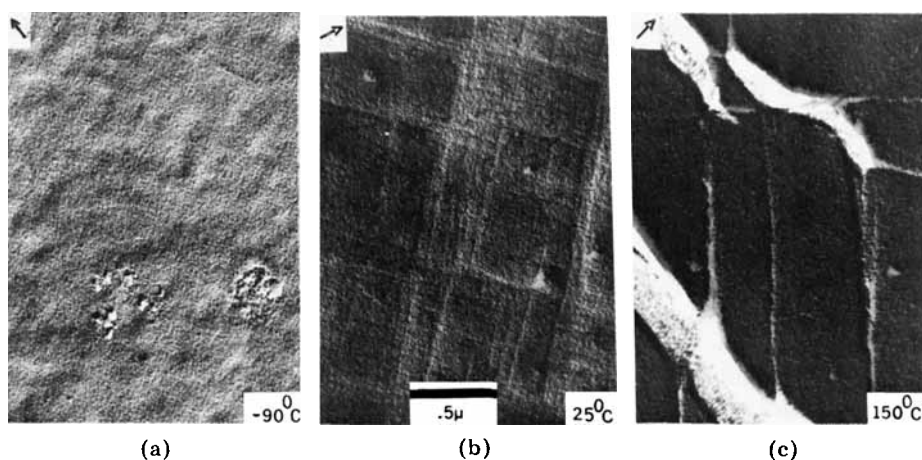

| (a) | (b) | (c) |

Fig. 6.   High-temperature shear to craze transition in 3000-Å-thick 2PPPO film.   Films deformed 10% (Pt–C shadowed at 30° angle, C coated).

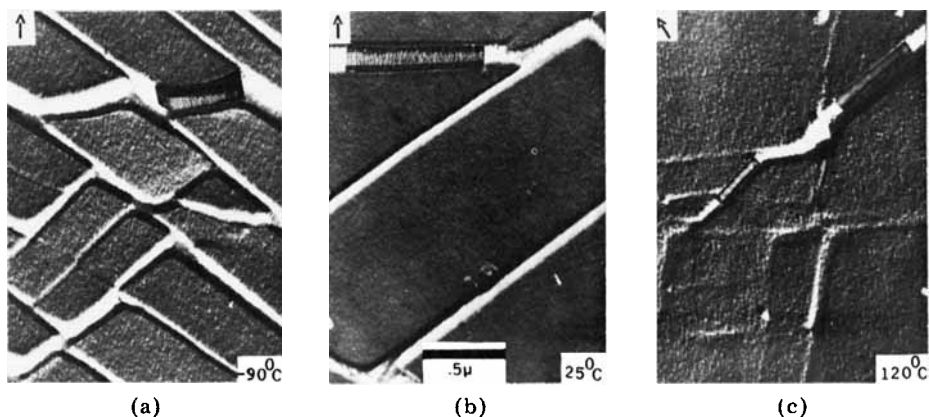

| (a) | (b) | (c) |

Fig. 7. Same as Figure 6, except that sharp shear banding and crazing is shown in MPPPO films.

also considerably less than the symmetrically substituted materials.[31]   These results suggest that the intermolecular packing determined by side group interactions is a factor in determining whether a polymer glass will behave as type I or type II.

Shear-to-Craze Transition–Effect of Blend Composition, Tacticity, and Molecular Weight

Blend composition has a large effect on the microdeformation observed in compatible PS–2MPPO glasses.   Thin films (ca. 3000 Å thick) of 2MPPO–PS blends show an interesting change in behavior at 20–30 wt-% of 2MPPO where a transition from type I to type II behavior takes place (Fig. 8).   Well-developed crazes are found only in the polymer with the lowest 2MPPO content, Figure 8(a), arrow C; at higher 2MPPO contents, crazes grow only a short distance before they bifurcate into shear band structures, Figure 8(b), arrow C.   Blends containing 30% 2MPPO do not craze at room temperature, Figure 8(c).

As the 2MPPO weight percent increases there is a greater propensity to form more diffuse bands, Figures 8(a)–8(c), arrows D, at the expense of sharp shear bands, Figures 8(a) and 8(b), arrows S.   The tendency to form these larger diffuse shear bands decreases with increasing 2MPPO content.

Comparison of Figures 9(a) and 8(b) with Figures 9(b) and 8(a) shows that a decrease in the temperature of deformation favors localization of the shear deformation in blends with a high percentage of PS.   The blend containing 20% 2MPPO undergoes a shear-to-craze transition above −90°C while 100% and 90% PS craze at −90°C.

Figure 10 summarizes the mechanical properties of 3000-Å-thick blend films. The lower dotted line refers to the shear-to-craze transition while the upper dotted line defines the transition from inhomogeneous to macroscopically "ho-

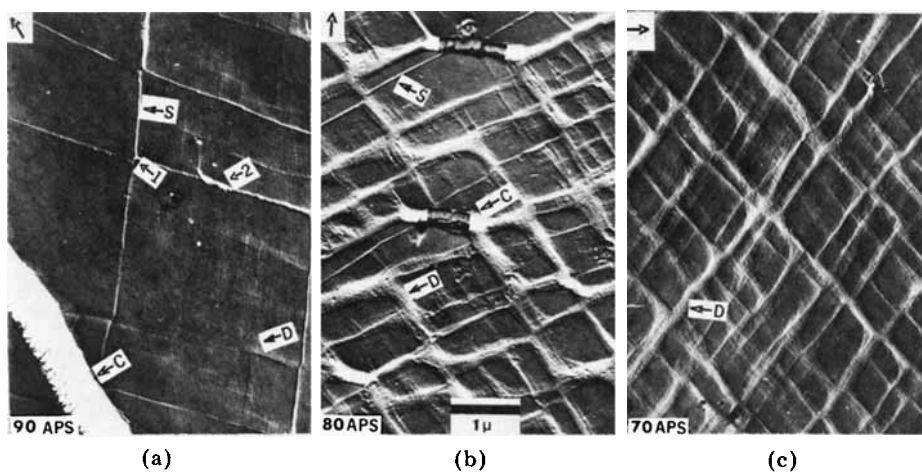(a)   (b)   (c)

Fig. 8. Shear-to-craze transition in 3000-Å-thick blend films—the effect of composition. Films deformed 10% at 25°C (Pt–C shadowed at 30° angle, C coated, arrow parallel to the maximum principal strain direction).
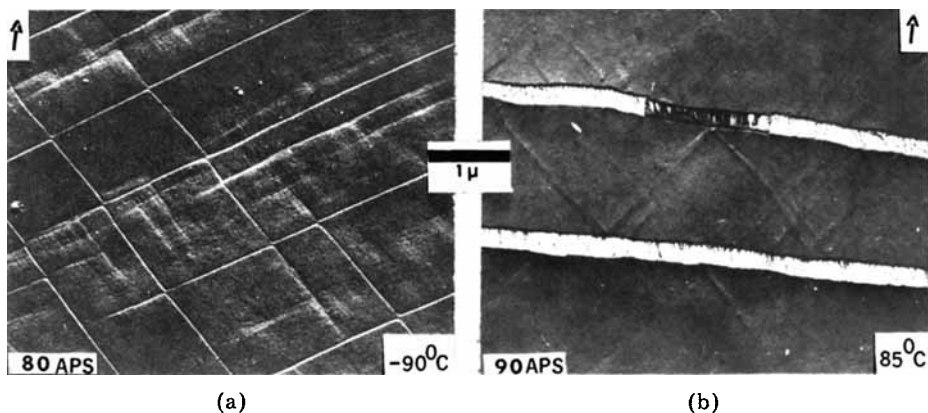
Fig. 9. Shear-to-craze transition in 3000-Å-thick blend films–the effect of deformation temperature. Films deformed 10% at the temperature indicated in the insert (Pt–C shadowed at 30° angle, C coated).
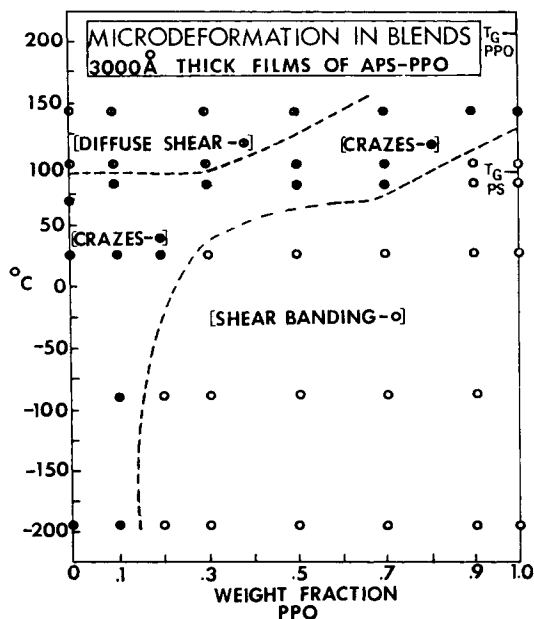

Fig. 10. Summary of effect of deformation temperature and composition on the microdeformation morphology in APS–2MPPO blends.

mogeneous" deformation that occurs at the T_g. This figure clearly represents the sharp change from type I ahd type II glass occurring at 20–30% 2MPPO.

APS (M_w = 2,000,000) and IPS (M_v = 2,000,000)–2MPPO blends were made in order to determine the effect of molecular weight and PS tacticity upon the blend mechanical properties. Table I summarizes the deformation morphology observed in the transition region (10–30% 2MPPO) as a function of molecular weight and tacticity in thin 3000-Å films.

A large difference in PS molecular weight has little effect on either the shear band or craze nucleation in the transition region. However, the tacticity of the PS component has a much larger influence upon the morphology. Although the

TABLE I
Summary of Microdeformation Morphology Found in 3000-Å-Thick 2MPPO–PS Blend Films
in the Type I–Type II transition region[a]

Composition tacticity	Molecular weight	Diffuse bands	Sharp bands	Crazes	Deformation temperature, °C
90 APS	2,000,000	dense	sparse	dense l.	25
	37,000	dense	sparse	dense l.	
90 IPS	2,000,000	none	dense	dense l.	25
80 APS	2,000,000	dense	sparse	sparse s.	25
	37,000	dense	sparse	sparse s.	
80 IPS	2,000,000	sparse	dense	sparse s.	25
70 APS	2,000,000	v. dense	none	none	25
	37,000	v. dense	none	none	
70 IPS	2,000,000	dense	dense	v. sparse s.	25
90 APS	2,000,000	sparse	v. dense	sparse s.	−90
	37,000	sparse	v. dense	sparse s.	
90 IPS	2,000,000	none	v. dense	dense s.	−90
80 APS	2,000,000	dense	dense	none	−90
	37,000	dense	dense	none	
80 IPS	2,000,000	none	v. dense	dense s.	−90
70 APS	2,000,000	v. dense	sparse	none	−90
	37,000	v. dense	sparse	none	
70 IPS	2,000,000	none	v. dense	sparse s.	−90

[a] v. = Very; l. = craze length >2–3 μ, s. = craze length < 2–3 μ.

shear-to-craze transition occurs at about the same composition (ca. 30% 2MPPO) at room temperature for both tacticities, the IPS blends deform by the sharp shear banding mechanism to a much greater extent than APS blends. This difference in shear band morphology is most noticeable at −90°C. Moreover, at this lower temperature, IPS blends show a slightly higher propensity to develop crazes.

IPS and APS–2MPPO blend films 10,000–15,000 Å thick undergo the transition from type I to type II behavior at higher 2MPPO contents of 30–50% (Figs. 11 and 12). The crazing process is little affected by the tacticity of the PS component; however, the shear band morphology is influenced. Although the concentration of diffuse shear zones increases with higher 2MPPO content, sharp shear bands can still form in the 30% IPS blend, Figure 12(c), and to a lesser extent in the 15% IPS blend. Only diffuse shear zones are found in APS blends containing greater than 50% 2MPPO. Tacticity has the same effect on shear band morphology at −90°C in these thick films.

Sharp and Diffuse Shear Morphologies and Their Interrelationship

Crazes and sharp shear bands both must be considered precursors to brittle failure modes since both contain a large localized strain.[13,32] Inspection of the shear displacements that sharp bands undergo when they intersect each other indicates that very high shear strains ($\gamma \cong 1.5$) are localized within these structures, see Figure 8(a), arrow 1, and Figure 12(b), arrow 1.[33] The shearing of both bands at their intersection implies that shear deformation had taken place within these bands subsequent to the time of their meeting.[33] The strain localized within these bands is so high that considerable internal voiding is often observed.
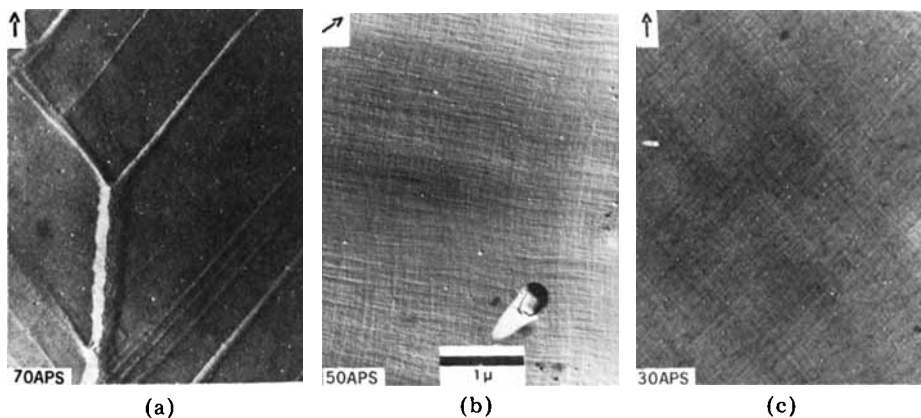
Fig. 11. Pt–C replicas of shear band and craze morphology in ca. 10,000-Å-thick films of 2MPPO–APS blends. Diffuse shear banding is predominant at high 2MPPO contents. Films deformed 10% at 25°C (Pt–C shadowed at 30° angle, C coated).
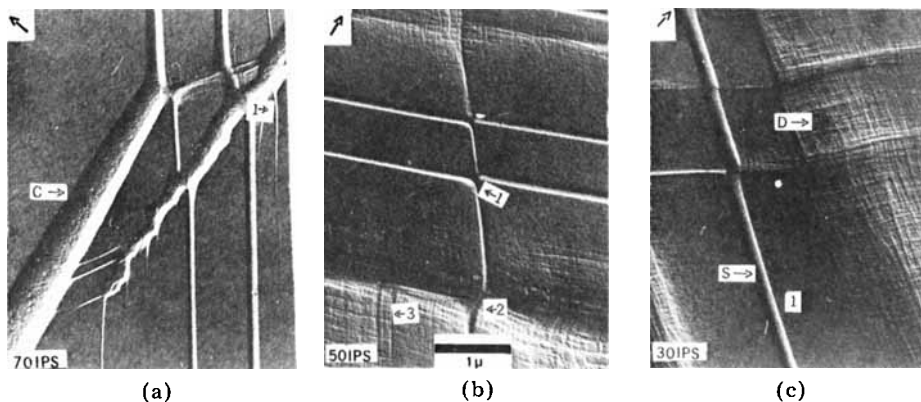

Fig. 12. Same as Figure 11, except 2MPPO-IPS blends. Sharp shear banding is found even at high 2MPPO contents.

It is well known that the sharp bands do not grow along the maximum shear stress direction.[34] Most of the bands formed in our films grow at 54 to 58° to the maximum principal stress direction. At these angles a considerable normal stress acts across the faces of the band.[35] The magnitude of the Pt–C shadow at one edge of the band and the shadow pileup at the opposite face implies that micronecking is taking place. The normal stress is undoubtedly responsible for the micronecking and voiding found within these bands, see Figure 8, arrow 2.

Figure 12(a), arrow 1, provides an especially clear example of the shear band growth sequence. Shear band 1 is obviously nucleated by the stress concentration ahead of the growing craze. The Pt–C shadow length indicates that the width of the band and the micronecking increases continuously from the shear band tip to the initiation point at the craze. The larger shear bands we observe develop from these smaller bands by a continuous shearing and micronecking process which draws more material from the surrounding matrix into the band. At a certain distance from the band tip the band width and micronecking undergo no further changes.

The 10,000–15,000-Å-thick films (Figs. 11 and 12) show a large distribution of bandwidths (50–2000 Å). Only relatively narrow (50–300 Å) sharp bands grow in 3000-Å-thin films (Fig. 8). The reason for this large dependence of bandwidth upon film thickness is not clear. Crazes have also been found to grow thicker as the film thickness increases, compare Figure 12(a) and Figure 8(b). This effect has been explained in a previous article.[24]

The large areas of diffuse shear actually consist of a highly packed collection of nascent sharp bands. Li and Wu have also recognized this morphological feature.[33] The diffuse bands clearly develop after the larger sharp bands. This sequence of nucleation is obvious from inspection of Figure 12(a) and Table I. Further evidence is found in Figure 12(b), arrow 2, where the sharp shear band is distorted by the diffuse shear band but not vice versa. A considerable region of shear stress relaxation surrounds each of the larger sharp bands, Figure 12(c), region 1. The growth of diffuse shear structures is retarded significantly by this stress attenuation. The larger bands were undoubtedly nucleated at structural inhomogeneities well below the yield point.

The very fine bands that make up the diffuse shear zones evidently nucleate so close to the same stress level that the preferential growth of any one of them is unlikely. Small bands of both shear orientations are nucleated immediately adjacent to each other. Unlike the much larger shear bands the fine bands do not noticeably shear each other at their intersection. Arrow 3, Figure 12(b), shows a small band that propagates through numerous other fine bands without being noticeably affected. This observation implies that shear deformation within the fine bands ceases soon after nucleation.

In thinner films especially, the diffuse shear zones tend to form a band structure. The maximum width of these diffuse bands is about the same as the film thickness. Once the band has grown to this width it can yield further in plane stress by a neck-down process.[35,36] The Pt–C shadowing in Figures 8(b) and (c) reveals that such a micronecking is occurring within the large diffuse bands. Plane stress yielding takes place at a lower stress level than plain strain yielding. Therefore, shear strain tends to concentrate within these diffuse bands. As expected, the diffuse bands that grow in thicker films are wider and less well defined, Figures 12(b) and (c). This plane stress yielding process would increase the ductility of thin films relative to thicker ones, which must deform in plane strain.

Strain Localization Within Crazes—Effect of Chemical Structure and Blend Composition

Gold particles were evaporated onto PC and PS film surfaces prior to deformation in order to qualitatively characterize the strain localized within the crazes that develop in these films. Figure 13 shows that less strain is concentrated both at the craze tip and within the more mature regions of PC crazes even though the degree of polymerization is lower and the deformation temperature is higher than in the PS sample. At 125°C there is no significant difference between the strain localized within PC crazes of MW 11,000 and 40,000.

Comparison of Figures 13(a) and 13(b) and Figures 14(a) and 14(b) shows that there is a difference between the cavitation process in PC and PS crazes. Even at temperatures very close to the T_g, PC crazes seem to be more stable with re-
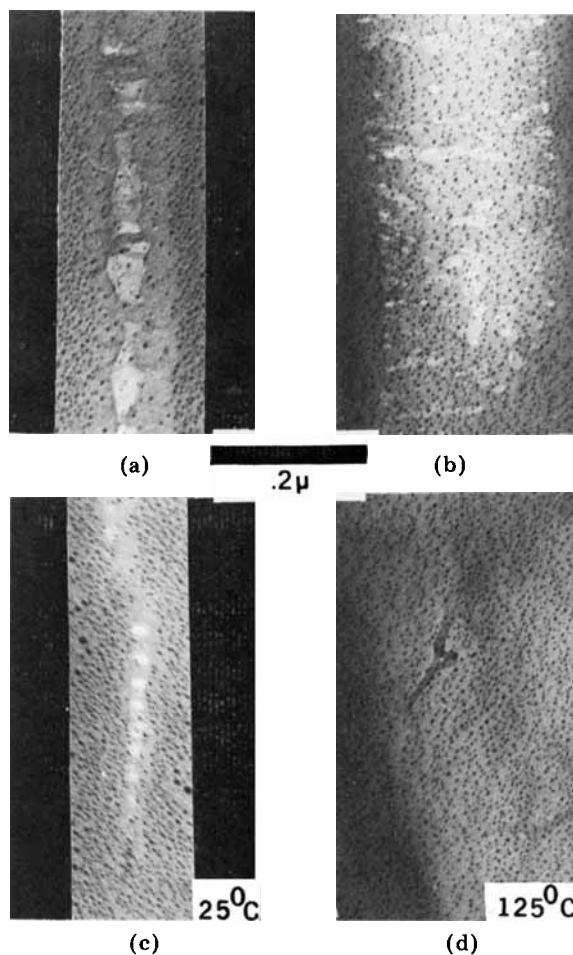
Fig. 13. Comparison of strain localized in PC and PS crazes (Au decorated prior to deformation, C coated): (a) and (b) mature regions of MW 97,000 PS and MW 40,000 PC, respectively; (c) and (d) initiation regions of PS and PC crazes, respectively.

spect to cavitation than PS crazes as a consequence of the greater strain delocalization in PC. Voids generally grow to a smaller size in PC, and a well-developed fibrillar structure is not apparent.

These observations are in agreement with the Pt–C shadowing results, which show that more craze nuclei contribute to the craze growth in the maximum principal strain direction in PC than in PS. The delocalization of the strain within the PC craze is undoubtedly why high-temperature PC crazes do not nucleate cracks or impede shear yielding.[1]

The transition from type I to type II behavior in 2MPPO–PS blends also involves a change of the strain localized within crazes. Figures 15(a) and (b) show examples of type I glasses which have a large amount of strain localized within their crazes. Type II glasses are shown in Figures 15(c) and (d); the relatively high density of gold particles present within these crazes is indicative of a smaller strain localization.
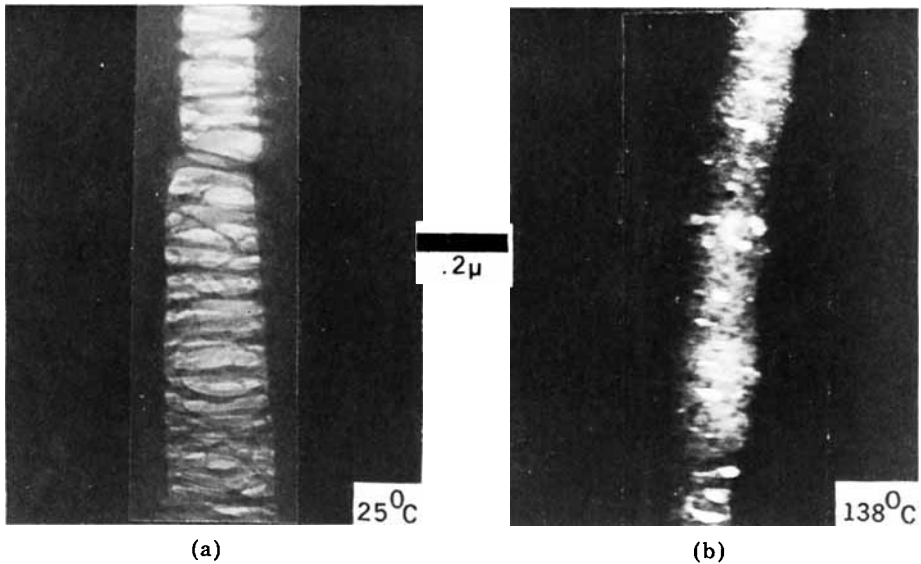
Fig. 14. Comparison of void structure in PS and PC crazes (C coated):   (a) MW 97,000 PS; (b) MW 40,000 PC.

Isolated ca. 300-Å craze nuclei appear in the 90% APS blend, Figure 15(a), dotted boxes.   This type of surface instability is typical in a type I glass deformed near its T_g.[24]   Type II glasses, Figures 15(c) and 15(d), do not appear to develop this morphology.

Surface Nodular Structure in PC Effect of Annealing and Deformation

The ca. 150-Å nodular structure present in the ½-hr annealed PC glass grows to 300 Å upon annealing for 60 hr, Figures 16(a) and 16(b).   The ca. 150-Å nodules organize into a lamellar row structure oriented perpendicular to the stretch direction upon 20% tensile deformation, Figure 16(c).   A 200–300-Å nodular structure is still present in the 60-hr annealed glass that has been deformed 20%, Figure 16(d).   However no row structure is apparent.

A particularly striking example of surface nodular development is found in Figure 17.   A deformation of 10% at 85°C induces the original 150-Å nodules to grow to ca. 400 Å in size.   Numerous diffuse shear bands can be found passing through the nodular field in Figure 17(a), arrows D.   A higher-magnification micrograph in the vicinity of one of the shear bands reveals that the morphology of the nodules within the shear band is not significantly different from those in the surrounding matrix, Figure 17(b), box.

It is unlikely that the nodular morphology found in Figure 17 can be completely attributed to etch pits in the vicinity of the fine shear bands.[33]   If this were the case the nodule size would change significantly at the diffuse shear band where the fine band concentration is highest.   Increased ordering of polymer chains upon deformation at high temperatures might account for the increased nodular size found in Figure 17.   In any case all the evidence suggests that the surfaces of PC glasses exhibit a significant chain packing heterogeneity on the 100–400-Å-size scale both before and after small plastic deformations.
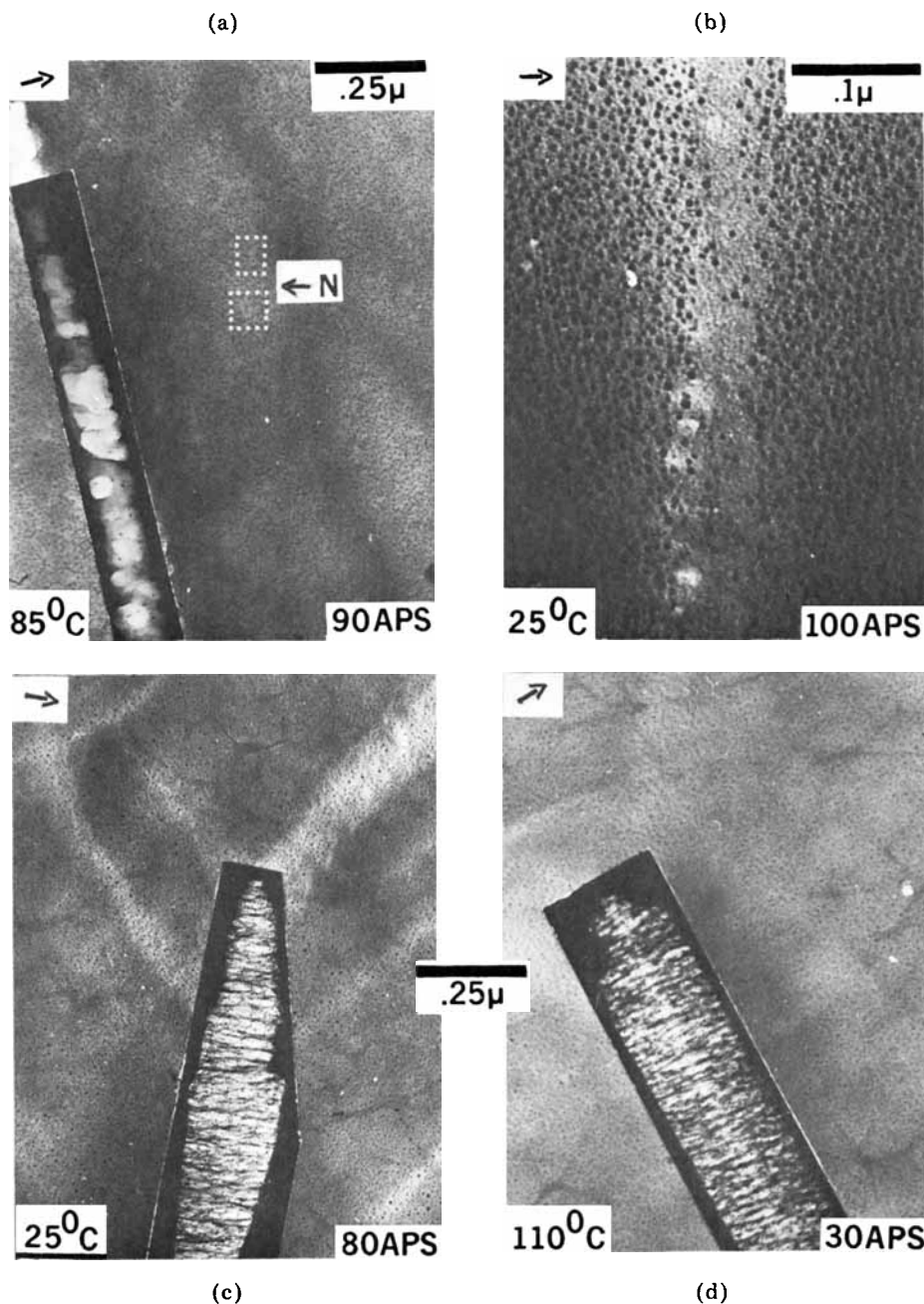
Fig. 15. Effect of deformation temperature and composition on strain localized within crazes. 3000-Å-Thick films gold decorated prior to 10% deformation.

According to Argon,[37] the localized dilational yield that is required for the nucleation of crazes depends upon the presence of packing heterogeneities in the glass. He suggests that shear yielding first ensues in a region of stress concentration localized in a poorly packed region situated between regions of higher packing density (e.g., nodules). The ca. 10–50-Å microshear band continues
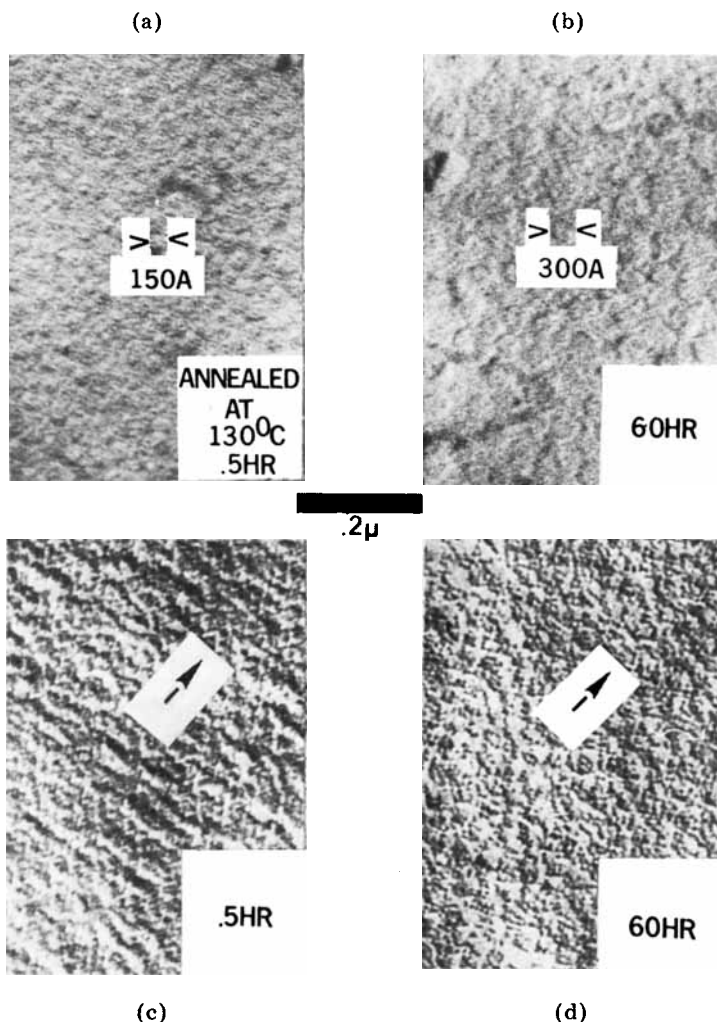
(a)   (b)

.2µ

(c)   (d)

Fig. 16. Effect of annealing upon surface nodular structure in MW 40,000 PC (Pt–C shadowed at 30° and C coated after NaOH etch): (a) and (b) undeformed; (c) and (d) deformed 20% at 25°C.

to grow until the higher shear resistance of the more closely packed region stops its development. Subsequently, a significant dilational stress concentration is localized at the heterogeneity. At this point the ca. 10-Å microvoiding necessary for craze nucleation could occur.[24]

In the framework of Argon's model, an increase in the packing density difference between the nodules and internodular regions in the surface would increase the dilational stress concentration. Annealing PC below the T_g increases the nodular size and most probably the difference in packing density between the ordered and less ordered regions. Conceivably this mechanism could explain the greater crazing propensity of the annealed glass.

However, ultimately, well-packed nodules might retard the development of large local plastic deformations. A mechanism of this type could explain the relatively smaller strain localization present in PC crazes as compared to PS crazes.
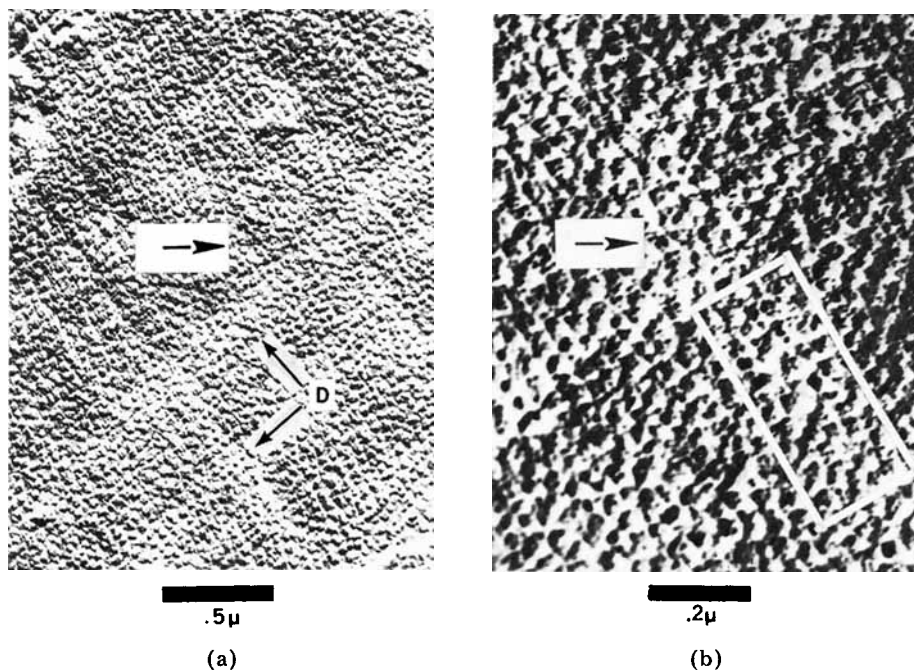
.5 μ .2 μ

(a) (b)

Fig. 17. (a) Nodular size enhancement upon 10% deformation at 85°C of a ½-hr 130°C annealed PC. (b) Higher magnification of Figure 17(a) showing that the nodular size is not affected by the presence of a diffuse shear band.

Dynamic Mechanical Properties of Blend Films

The anelastic spectra of APS and IPS–2MPPO blends were obtained in order to ascertain the molecular mechanisms controlling the strain localized within shear band structures. Figure 18 shows that when only 15 wt-% IPS is added to 2MPPO, the broad low-temperature β peak of 2MPPO is almost completely suppressed. Generally, the same amount of low molecular weight diluent must be added to polycarbonate of bisphenol A (PC) and polyvinyl chloride (PVC) in order to eliminate the β relaxation in these materials.[6] This implies that PS and 2MPPO approach segmental compatibility. Other workers have recently come to the same conclusion.[38]

The β relaxation of symmetrically disubstituted PPOs has been attributed to a hindered oscillation of the phenylene ring about the ether oxygen. All type II polymers have this low-temperature main-chain relaxation. IPS packs so well with 2MPPO that small amounts of IPS virtually eliminate low-temperature backbone motions in 2MPPO. As a consequence, the low-temperature shear modulus increases rapidly with increasing PS content (Fig. 18).

APS also suppressed the β relaxation of 2MPPO but not to the same extent as IPS (Fig. 19). Even though APS shows a much greater tendency to develop diffuse shear bands, it is questionable whether this morphological difference can be completely attributed to changes in the β peak intensity. For instance, PC can undergo significant changes in shear band morphology while its β peak remains unaffected.[10]

The anelasticity of PPO increases slightly above 300°K into a very broad relaxation (Fig. 18). The intensity of this intermediate process is considerably
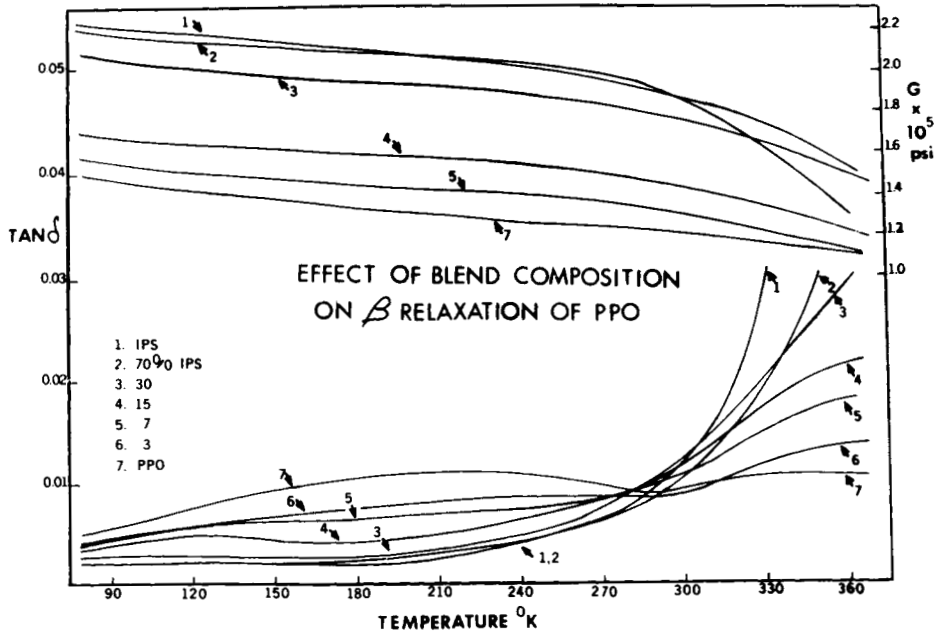
Fig. 18. Effect of blend composition on the β and intermediate transitions of 2MPPO.
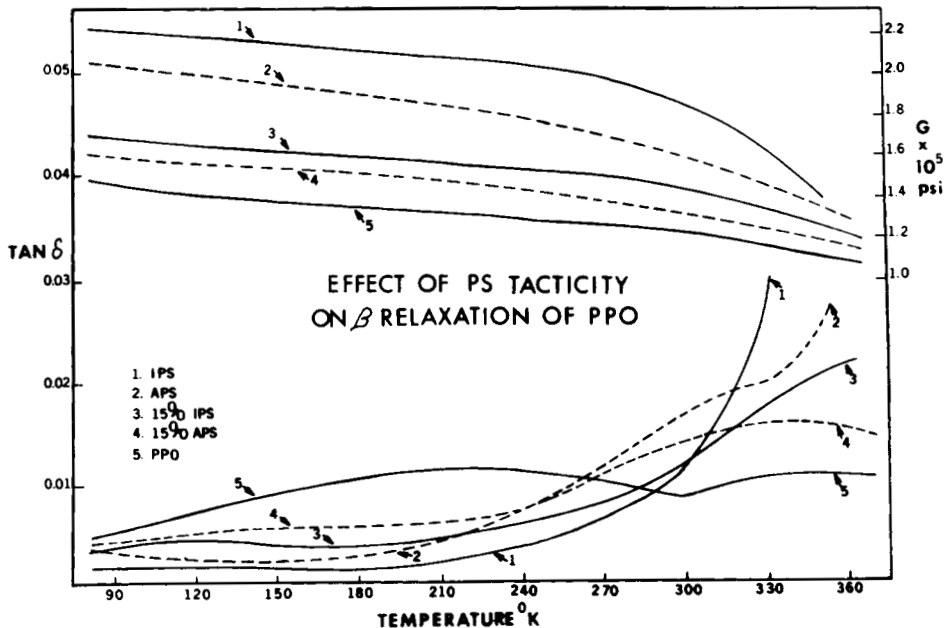

Fig. 19. Comparison of effect of APS and IPS on the anelastic spectrum of PS-2MPPO blends.

enhanced by even small amounts of IPS. The maximum of the peak lies above 370°K (the maximum use temperature of our torsion pendulum). Blending with APS decreases the temperature of this peak to 340°C (Fig. 19). The low concentration of APS makes it unlikely that this high-temperature relaxation is its intermediate relaxation. Other workers have also observed an enhancement of the 2MPPO intermediate transition upon blending with APS.[38]

The high-temperature 2MPPO relaxation in the IPS blend is more intense than in a blend containing an equivalent amount of APS. The intensity of the peak in IPS–2MPPO could have been enhanced by the quenching treatment the polymer was given[19] (APS– 2MPPO was slow cooled). Slow cooling of the IPS blend would undoubtedly move this transition to a higher temperature and decrease its intensity,[8] even further differentiating the 15% APS and 15% IPS anelastic spectra.

Relationship Between Microstructure and Deformation Morphology

Ultraviolet and Fourier transform infrared measurements[40] have shown that the conformational energy of the 2MPPO chain is increased when it is mixed with PS. This increase in energy is greater for APS blends than IPS blends at the same composition. Bach Van and Noel[39] have concluded that an increase in the configurational energy of the polymer chain decreases the temperature of the intermediate transition and increases its intensity. The spectroscopic and dynamic mechanical results on the blends are consistent with this hypothesis. An increase in the clnformation energy of the chain can be identified with an increase of the glass enthalpy which increases the propensity of the glass to deform by diffuse shear banding.[10,33]

However, 2MPPO and PS have a negative excess volume of mixing and are segmentally compatible due to a strong phenyl–phenylene ring interaction.[40] Since the β relaxation is though to involve motions in isolated, poorly packed regions,[41] the strong 2MPPO–PS interaction could be responsible for the suppression of the 2MPPO β peak by small amounts of PS. Sharp shear banding would be favored by improved packing[42,43] and a decrease in low-temperature anelasticity.

The observed microshear band morphology must be a consequence of the balance between an increase in conformational energy and an improvement in intermolecular bonding and packing upon blending with PS. APS blends shear in a more delocalized fashion relative to IPS blends because of a higher conformational energy at the same blend composition.

The transition from type II to type I crazing behavior that occurs at high PS contents is not well correlated with the changes that occur in the low-temperature dynamic mechanical spectrum. Only small amounts of 2MPPO (20–30%) are required for the transition from type I to type II. Shear mechanisms, whether diffuse or sharp, become more favored relative to crazing at this transiton. In the framework of Argon's theory,[15,16] the shear activation event in type II polymers involves the cooperative rearrangement of a bundle of adjacent chains (see Introduction). The activated state in type I usually consists of only one chain. The constraint of interchain cooperativity in the activated state significantly suppresses the nucleation of crazes in type II glasses.[15]

The strong bonding between and efficient packing of PS and 2MPPO chains might induce interchain cooperativity in glasses containing a sufficiently large number of PS–2MPPO interactions. The increase in the shear activation volume that is observed upon increasing the concentration of 2MPPO in PS–2MPPO blends lends support to this mechanism.[38] This hypothesis could be checked by detailed yield stress measurements on the blends in the vicinity of the transition composition. Analysis of the data according to Argon's theory[16] should

determine whether a transition from a single chain- to a many chain-activated state is occurring at this composition. Measurements under a compressive stress state would be required for the determination of the yield stress at high PS contents.

CONCLUSIONS

1. There are two types of amorphous polymer glasses: type I, which craze at all temperatures between T_g and $-195°C$; and Type II, which craze only in a narrow temperature regime immediately below T_g.

2. Vinyl polymers with sufficiently bulky and or polar side chains generally behave as type I polymers, while type II polymers include polyarylenes with flexible main-chain linkages.

3. Addition of ca. 30% 2MPPO to PS induces a transition from a type I to a type II glass. An increase in intrachain cooperativity due to a strong phenyl–phenylene ring interaction between 2MPPO and PS may be sufficient to suppress crazing in blends with more than ca. 30% 2MPPO.

4. A nodular surface structure in type II glasses may by responsible for the smaller strains localized within crazes in these glasses relative to type I glasses.

5. The β relaxation of 2MPPO is suppressed by the addition of small amounts of PS. On the other hand, the 2MPPO intermediate transition is enhanced and moved to lower temperatures.

6. The propensity for polymer glasses to form sharp shear bands at the expense of diffuse bands is enhanced by a decrease in the conformational energy of the polymer chain and an improvement in the glassy state packing.

References

1. J. Kastelic and Eric Baer, *J. Macromol. Sci.-Phys.*, **B7** (4), 679 (1973).

2. A. S. Hay, in *Encyclopedia of Polymer Science and Technology*, Vol. 10, H. Mark, Ed., Interscience, New York, 1969, p. 101.

3. S. Rabinowitz and P. Beardmore, *CRC Crit. Rev. Macromol. Sci.*, 1(1), 1 (1972).

4. P. Beardmore, *Philos. Mag.*, **19**, 389 (1969).

5. R. F. Boyer, in *Encyclopedia of Polymer Science and Technology*, Vol. 13, H. Mark, Ed., Interscience, New York, 1969.

6. N. Kinjo, *Jpn. Plast.*, 6 (Oct. 1973).

7. K. H. Hellwege, J. Hennig, and W. Knappe, *Kolloid-Z.*, **188**, 121 (1963).

8. M. G. Wysgoski and G. S. Y. Yeh, *J. Macromol. Sci.-Phys.*, **B10**(3), 441 (1974).

9. P. B. Bowden and S. Raha, *Philos. Mag.*, **22**, 455, 463 (1970).

10. S. E. B. Petrie, in *Polymeric Materials*, E. Baer and S. V. Radcliffe, Eds., ASM, Cleveland, 1975, p. 455.

11. C. Bauwens-Crowet, J. C. Bauwens, and G. Homes, *J. Polym. Sci.*, A-2, **7**, 735 (1972); *J. Mater. Sci.*, **7**, 176 (1976).

12. K. H. Illers and H. Breuer, *J. Colloid Sci.*, **18**, 1, (1963).

13. A. S. Argon, R. D. Andrews, J. A. Godrick, and W. Whitney, *J. Appl. Phys.*, **39**, 1899 (1968).

14. P. B. Bowden and J. L. Henshall, unpublished results, 1973.

15. A. S. Argon and M. I. Bessonov, *Philos. Mag.*, (1976).

16. A. S. Argon, *Philos. Mag.*, **28**, 839 (1973).

17. S. H. Carr, P. H. Geil, and E. Baer, *J. Macromol. Sci.-Phys.*, **B2**(1), 13 (1968).

18. J. J. Klement and P. H. Geil, *J. Macromol. Sci.-Phys.*, **B6**(1), 31 (1972); *ibid.*, **B5**, 505, 535 (1971).

19. K. Neki and P. H. Geil, *J. Macromol. Sci.-Phys.*, **B8**(1–2), 295 (1973).

20. R. J. Morgan and J. E. O'Neal, *J. Ploym. Sci.*, **14**, 1053 (1976).

21. G. S. Y. Yeh, *J. Macromol. Sci.-Phys.*, **B6**(3), 451 465 (1962); also in *CRC Crit. Rev. Macromol. Sci.*, **1**(2), 173 (1972).

22. R. G. Kirste, W. A. Kruse, and K. Ibel, *Polymer*, **16**, 120 (1975).

23. J. H. Wendorff, E. W. Fischer, D. Dentenmaien, G. Fiesen, and I. Voigt - Martin, *Prepr. Am. Chem. Soc., Div. Polym. Chem.*, **15**(2), 8 (1974).

24. S. Wellinghoff and Eric Baer, *J. Macromol. Sci.-Phys.*, **B11**(3), 367 (1975).

25. E. L. Thomas and S. J. Israel, *J. Mater. Sci.*, **10**(9), 1603 (1975).

26. S. Wellinghoff and E. Baer, *Prepr. Am. Chem. Soc., Div. Org. Coat. Plast. Chem.*, **36**(1), 140 (1976).

27. W. M. Prest, Jr. and R. S. Porter, *J. Poly. Sci. (A-2)*, **10**, 1639 (1972).

28. W. J. MacKnight, Lecture presented at CWRU, Cleveland, 1975.

29. A. Eisenberg and B. Cayrol, *J. Polym. Sci.*, **C**(35), 129 (1971).

30. B. Cayrol, A. Eisenberg, J. F. Harrod, and P. Rocaniere, *Macromolecules*, **5**(6), 676 (1972).

31. A. Tonelli, *Macromolecules*, **6**(4), 503 (1973).

32. R. P. Kambour, *Macromol. Rev.*, **7**, 1, (1973).

33. J. B. C. Wu and J. C. M. Li, *J. Mater. Sci.*, **11**(3), 434 (1976).

34. A. S. Argon, in *Polymeric Materials*, E. Baer and S. V. Radcliffe, Eds., ASM, Cleveland, 1975, p. 441.

35. P. B. Bowden, in *The Physics of Glassy Polymers*, R. N. Haward, Ed., Wiley, New York, 1973, p. 279.

36. J. G. Williams, *Stress Analysis of Polymers*, Longmans, London, 1973, p. 255.

37. A. S. Argon, Presented as Main Lecture in Marianske Lazne, Czechoslovakia, Sept. 2–5, 1974, at Fourth Discussion Conference on Macromolecules entitled "Heterogeneities in Polymers," to be published by Butterworth, B. Sedlacek and B. C. L. Weedon, Eds.

38. A. F. Yee, *Polym. Prepr., Am. Chem. Soc., Div. Polym. Chem.*, **17**(1), 145 (1976); *Polym. Eng. Sci.*, **17**(3), 213 (1977).

39. N. Bach Van and C. Noel, *J. Polym. Sci., Chem. Ed.*, **14**(7), 1627 (1976).

40. S. Wellinghoff and E. Baer, *J. Polym. Sci., Phys. Ed.*, **15**(11), 1913 (1977).

41. G. P. Johari, *J. Chem. Phys.*, **58**(4), 1766 (1973).

42. H. B. Hopfenberg, V. T. Stannett, and G. M. Folk, *Polym. Eng. Sci.*, **15**(4), 261 (1975).

43. M. H. Litt and A. V. Tobolsky, *J. Macromol. Sci.-Phys.*, **B1**(3), 433 (1967).

44. E. P. Cizek, U.S. Pat. 3,383,435 (May 14, 1968).

45. C. B. Bucknell, D. Clayton, and W. E. Keast, *J. Mater. Sci.*, **7**, 1443 (1972).